Available online at www.sciencedirect.com

ScienceDirect

IFAC Papers Online CONFERENCE PAPER ARCHIVE

IFAC PapersOnLine 53-2 (2020) 7305–7311

Flocking of Linear Parameter Varying Agents: Source Seeking Application with Underwater Vehicles

Aly Attallah * **Adwait Datar** * **Herbert Werner** *

* *Institute of Control Systems, Hamburg University of Technology, Eissendorfer Str. 40, 21073 Hamburg, Germany (e-mail: {aly.attallah, adwait.datar, h.werner}@tuhh.de)*

Abstract: A distributed flocking control scheme is proposed for a network of Autonomous Underwater Vehicles (AUVs) which are modeled as Linear Parameter Varying (LPV) systems. This scheme is applied here to the solution of a source seeking problem, i.e. the vehicles (agents) measure the local values of a scalar field and are required to flock to its maximum (source). It is assumed that agents have the gradient and Hessian information of the scalar field at their current position. The control architecture of each agent is divided into two modules: a flocking filter which receives data from neighbours and generates a reference signal based on a flocking control law, and a feedback loop for tracking this reference. By this approach, a separation in design is achieved by designing a local LPV tracking controller for each agent and a network flocking filter which can be analyzed to guarantee stability in the sense of Lyapunov, i.e. the boundedness of agents' trajectories. Simulation results illustrate the practicality and benefits of the proposed flocking architecture scheme by applying it to a network of realistic autonomous underwater vehicles.

Keywords: Linear parameter-varying systems, non-holonomic vehicles, distributed nonlinear control, tracking.

1. INTRODUCTION

Over the last several years, multi-agent systems research has attracted the interest of researchers in both civil and military applications due to its ability of performing missions in shorter time and high precision in comparison with a single agent (Leonard and Fiorelli, 2001), (Olfati-Saber, 2006) and (Fax and Murray, 2004). One interesting application of multi-agent systems is the source seeking problem that is defined as the localization of an origin of, for example, a toxic cloud in the air or an oil spill in the sea. The concentration levels of this kind of pollution can be represented by a scalar field. Swarms of agents, equipped with suitable sensors, can provide an efficient way of localizing source of such concentration levels.

A major part of the literature on source seeking problems focuses on formation control (with a first order consensus protocol) or flocking (a type of second order consensus), and considers agents modeled as LTI systems. A solution based on a combination of formation control and gradient estimation is proposed in (Rosero and Werner, 2014) for a group of identical LTI agents. In (Barogh et al., 2015) a distributed gradient estimation scheme is used by a swarm of nonholonomic robots to maintain a specified formation around the source. A source seeking problem in three dimensional space for a group of aerial vehicles is studied in (Soares et al., 2016), and solved again based on formation control. A degree of flexibility is achieved when solving the problem using the flocking rules *cohesion, separation, velocity alignment*, while moving towards a target or source, which leads to a fluid-like motion of the agents. In (Turgeman et al., 2019), a glowworm optimization based flocking algorithm is applied to second order LTI agents which ensure that they can locate an unknown field's extrema while staying together without collision.

When agents are subject to nonholonomic constraints, like fixed-wing unmanned aerial vehicles (UAVs) or autonomous underwater vehicles (AUVs) , then modelling them as linear parameter varying (LPV) systems has been shown to lead to efficient distributed gain-scheduled control schemes (Gonzalez et al., 2015).

Here we consider underwater pollution scenarios such as oil spills, and a flock of autonomous underwater vehicles that is employed to localize the source. For this purpose the *Hippocampus* micro underwater vehicle developed at TUHH (Solowjow et al., 2018) is used for controller design and in simulation. The contribution of this paper is twofold: first, modeling the *Hippocampus* as an LPV system, and design of an LPV tracking controller. And second the proposed structure of a flocking control network for a group of LPV agents that can be used for solving source seeking problems.

This paper is organized as follow. In Section 2, some background about graph theory and LPV output feedback controller synthesis is reviewed. LPV modeling of the *Hippocampus* vehicle and the local control loop architecture are presented in Section 3. Section 4 shows the proposed

10.1016/j.ifacol.2020.12.982

flocking network loop and presents an analysis result on boundedness of trajectories of LPV agents when they are cooperating in a flock. Simulation results for single agent trajectory tracking and for a source seeking scenario are presented in Section 5. Finally, in Section 6 conclusions are drawn.

2. PRELIMINARIES

Notation. We let I denote the identity matrix of appropriate size. Kronecker extensions of matrices or systems are denoted by $\hat{X} = I_n \otimes X$ and $M_{(n)} = X \otimes I_n$. The induced $\mathcal{L}_2$-norm of the LPV system $T_{zr}(\rho)$ with continuous time input signal $r(t)$ and output signal $z(t)$ and scheduling parameter vector $\rho \in \mathcal{P} \subset \mathbb{R}^{n_\rho}$ is defined as

$$\|T_{zr}(\rho)\|_{\mathcal{L}_2} = \sup_{\rho\in\mathcal{P}} \sup_{\|r\|_{\mathcal{L}_2}\neq 0} \frac{\|z\|_{\mathcal{L}_2}}{\|r\|_{\mathcal{L}_2}},$$

where $\mathcal{P}$ is a compact set of admissable parameter values.

We use concepts from graph theory to model the interconnections. Let $\mathcal{G} = (\mathcal{V}, \mathcal{E})$ be an undirected unweighted graph of order N with the set of nodes $\mathcal{V} = \{v_1, v_2, \dots v_N\}$, the set of edges $\mathcal{E} \subseteq \mathcal{V} \times \mathcal{V}$. The adjacency matrix $A \in \mathbb{R}^{N\times N}$ is given by $A = [a_{ij}]$ with 0 and 1 entries such that $a_{ij} = 1 \iff (v_i, v_j) \in \mathcal{E}$. Let d_i be the degree of node i, i.e., the number of links at that node and let $D \in \mathbb{R}^{N\times N}$ be a diagonal matrix formed by the d_i's along the diagonal. Define the graph Laplacian matrix $L \in \mathbb{R}^{N\times N}$ as $L = D - A$. We consider N agents living in an $m-$dimensional space and denote their positions and velocities by $q_i,\ p_i \in \mathbb{R}^m$, respectively. Let $q,\ p \in \mathbb{R}^{Nm}$ be constructed by stacking q_i's as $q = [q_1^T q_2^T \dots q_N^T]^T$ and $p = [p_1^T p_2^T \dots p_N^T]^T$.

We will make use of the flocking framework presented in (Olfati-Saber, 2006), in which the flocking control law is divided into three components: α-agents representing the interaction between agents, γ-agents representing mission goals for the flock, and β-agents for obstacle avoidance. Following (Olfati-Saber, 2006), we denote by $L(q)$, the state-dependent Laplacian matrix. The inter-agent potential function between agent i and j is denoted by Φ_{ij} and the potential for the complete system is then denoted by $V(q) = \frac{1}{2}\sum_{(i,j)\in\mathcal{E}} \Phi_{ij}$.

Let $F : \mathbb{R}^m \to \mathbb{R}$ be a smooth scalar field defined over space. The gradient $\nabla F(q_i) \in \mathbb{R}^m$ is defined by

$$\nabla F(q_i) = [\frac{\partial F(q_i)}{\partial q_i^1} \frac{\partial F(q_i)}{\partial q_i^2} \dots \frac{\partial F(q_i)}{\partial q_i^m}]^T.$$

By defining $\mathbf{F} : \mathbb{R}^{Nm} \to \mathbb{R}$ by $\mathbf{F}(q) = \sum_i F(q_i)$, we get

$$\nabla\mathbf{F}(q) = [\nabla F(q_1)^T \nabla F(q_2)^T \dots \nabla F(q_N)^T]^T.$$

The Hessian $\nabla^2\mathbf{F}(q_i)$ is defined as

$$[\nabla^2\mathbf{F}(q_i)]_{uv} = \frac{\partial^2 F(q_i)}{\partial q_i^u \partial q_i^v}.$$

Similarly overloading the notation for $F(q)$, we obtain

$$\nabla^2\mathbf{F}(q) = \text{blkdiag}\Big(\nabla^2 F(q_1), \nabla^2 F(q_2), \cdots, \nabla^2 F(q_N)\Big).$$

Let the scalar field F represent the distribution of the concentration over space and let the source be denoted by a point $q_s \in \mathbb{R}^m$ that minimizes $-F$. We can thus convert the source seeking problem into a distributed minimization problem.

We will draw upon concepts from optimization to motivate our source seeking protocol. As shown in (Alvarez et al., 2002), the dynamics of the continuous-time equivalent of the second order Newton-type method with momentum are represented by

$$\begin{aligned} \dot{x} &= v \\ \dot{v} &= -k_1(\nabla^2 F(x))\, v - k_2 \nabla F(x)\,. \end{aligned} \tag{1}$$

Motivated by this idea, we propose the control law for flocking γ-agents as

$$u^\gamma = -k_1 \nabla^2 F(q) p - k_2 \nabla F(q). \tag{2}$$

2.1 LPV Output Feedback Controller Design

This section reviews existing results on LPV output feedback controller synthesis, see (Wu, 1995) and (Wu et al., 1996). Consider an open-loop LPV system $G(\rho)$ defined as

$$\begin{bmatrix} \dot{x} \\ z \\ v \end{bmatrix} = \begin{bmatrix} A(\rho) & B_1(\rho) & B_2(\rho) \\ C_1(\rho) & 0 & D_{12}(\rho) \\ C_2(\rho) & D_{21}(\rho) & 0 \end{bmatrix} \begin{bmatrix} x \\ r \\ u \end{bmatrix} \tag{3}$$

$C_1(\rho) = \begin{bmatrix} C_{11}^T(\rho)\ C_{12}^T(\rho) \end{bmatrix}^T$, $B_1(\rho) = [\, B_{11}(\rho)\ B_{12}(\rho)\,]$, $D_{12} = [\, 0\ I\,]$, $D_{21} = \begin{bmatrix} 0^T\ I \end{bmatrix}^T$, $x \in \mathbb{R}^n, r \in \mathbb{R}^{n_r}, u \in \mathbb{R}^{n_u}, z \in \mathbb{R}^{n_z}$ and $v \in \mathbb{R}^{n_v}$.

Consider an LPV controller $K(\rho)$ of the form

$$\begin{bmatrix} \dot{x}_K \\ u \end{bmatrix} = \begin{bmatrix} A_K(\rho) & B_K(\rho) \\ C_K(\rho) & D_K(\rho) \end{bmatrix} \begin{bmatrix} x_K \\ v \end{bmatrix} \tag{4}$$

The controller generates the control input u. It depends linearly on the measurement v and has arbitrary dependence on the (measurable) parameter vector ρ. The closed-loop interconnection of $G(\rho)$ and $K(\rho)$ is given by a lower linear fractional transformation (LFT) and is denoted by $\mathcal{F}_l(G(\rho), K(\rho))$. The objective is to synthesize a controller $K(\rho)$ that minimizes the closed-loop $\mathcal{L}_2$ gain

$$\min_{K(\rho)} \|\mathcal{F}_l\left(G(\rho), K(\rho)\right)\|_{\mathcal{L}_2} \tag{5}$$

from performance input r to performance output z.

The following theorem provides a sufficient condition that forms the basis for LPV controller design.

Theorem 1. (Wu, 1995) Let $\mathcal{P}$ be a compact set and $G(\rho)$ a given LPV system. There exists a controller $K(\rho)$ such that $\|\mathcal{F}_l\left(G_\rho, K_\rho\right)\| \leq \gamma$ if there exist matrices $P = P^T > 0$ and $Q = Q^T > 0$ such that $\forall \rho \in \mathcal{P}$

$$\begin{bmatrix} P & I \\ I & Q \end{bmatrix} \geq 0$$

$$\begin{bmatrix} Q\bar{A}(\rho)^T + \bar{A}(\rho)Q - \gamma B_2(\rho)B_2(\rho)^T & QC_{11}(\rho)^T & B_1(\rho) \\ C_{11}(\rho)^T Q & -\gamma I & 0 \\ B_1(\rho)^T & 0 & -\gamma I \end{bmatrix} < 0$$

$$\begin{bmatrix} \tilde{A}(\rho)^T P + P\tilde{A}(\rho) - C_2(\rho)^T C_2(\rho) & PB_{11}(\rho) & C_1(\rho)^T \\ B_{11}(\rho)^T P & -\gamma I_{nd1} & 0 \\ C_1(\rho) & 0 & -\gamma I_{ne} \end{bmatrix} < 0$$

where $\bar{A}(\rho) := A(\rho) - B_2(\rho)C_{12}(\rho)$ and $\tilde{A}(\rho) := A(\rho) - B_{12}(\rho)C_2(\rho)$.

2.2 Problem statement

We consider a group of N nonholonomic mobile agents, the nonlinear dynamics of which are modeled as LPV systems

$G(\rho)$, and a scalar field F that models the concentration level of a pollutant. We assume that each agent i has access to its position q_i, velocity p_i, as well as to the local gradient $\nabla F(q_i)$ and local Hessian $\nabla^2 F(q_i)$ of the field. We further assume that each agent is equipped with communication capabilities so that it additionally knows the position q_j and velocity p_j of all its neighbors $j \in \mathcal{N}_i$. The problem is then to design a distributed control law that causes the agents located at arbitrary initial positions to flock towards the source of the scalar field.

We divide the problem into two sub-problems. We first design a local LPV tracking controller for each agent with a guaranteed $\mathcal{L}_2$ performance, and then design a flocking filter that maintains the stability of the overall networked system.

3. UNDER WATER VEHICLE LPV MODELING AND CONTROL

This section presents a quasi-LPV model of the *hippocampus* underwater vehicle, and the design of a gain-scheduled output feedback tracking controller.

3.1 Nonlinear Dynamics

The general nonlinear dynamics of autonomous under water vehicles are formulated in (Fossen, 2011) in North-East-Down inertial coordinates $\{\mathcal{I}\}$ with orthonormal vectors $\{i_N, i_E, i_D\}$ and in body-fixed coordinates $\{\mathcal{B}\}$ with orthonormal vectors $\{x_B, y_B, z_B\}$ centered at body center of gravity, see Fig. 1.

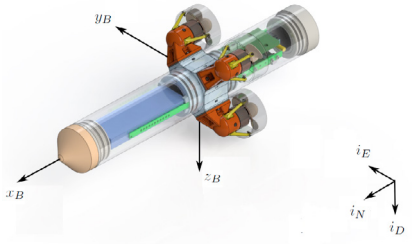

Fig. 1. *Hippocampus* with Inertial and Body coordinates

Based on nomenclature used in (Fossen, 2011), position and orientation are combined into the vector $\eta = [N\ E\ D\ \phi\ \theta\ \psi]^T$, and linear and angular velocities are combined into the vector $\nu = [u\ v\ w\ p\ q\ r]^T$. The dynamics of the *Hippocampus* vehicle is controlled by four propellers that produce the thrust force and moments which are combined into the vector $\tau = [f\ 0\ 0\ \tau_\phi\ \tau_\theta\ \tau_\psi]^T$. A nonlinear state space model of underwater vehicle is then

$$\begin{bmatrix}\dot{\eta}\\ \dot{\nu}\end{bmatrix} = \begin{bmatrix}0 & J(\eta)\\ -M^{-1}G(\eta) & -M^{-1}(C(\nu)+D(\nu))\end{bmatrix}\begin{bmatrix}\eta\\ \nu\end{bmatrix} + \begin{bmatrix}0\\ M^{-1}\end{bmatrix}\tau, \quad (6)$$

where $J(\eta) = blkdiag(\mathcal{R}, \mathcal{T})$ is block diagonal matrix of the rotational tensor $\mathcal{R}$ and the angular velocity transformation tensor $\mathcal{T}$ such that

$$\mathcal{R} = \begin{bmatrix} c_\psi c_\theta & -s_\psi c_\phi + c_\psi s_\theta s_\phi & s_\psi s_\phi + c_\psi c_\phi s_\theta \\ s_\psi c_\theta & c_\psi c_\phi + s_\phi s_\theta s_\psi & -c_\psi s_\phi + s_\theta s_\psi c_\phi \\ -s_\theta & c_\theta s_\phi & c_\theta c_\phi \end{bmatrix}$$

$$\mathcal{T} = \begin{bmatrix} 1 & s_\phi t_\theta & c_\phi t_\theta \\ 0 & c_\phi & -s_\phi \\ 0 & s_\phi/c_\theta & c_\phi/c_\theta \end{bmatrix}$$

where $c., s., t.$ stand for $\cos(\cdot), \sin(\cdot), \tan(\cdot)$.

$G(\eta)$ represents the hydrostatic load and is defined as

$$G(\eta) = diag\Big(0, 0, 0, z_g \mathrm{m} g c\theta sinc(\phi), z_g \mathrm{m} g sinc(\theta), 0\Big)$$

where m is the *Hippocampus* mass and g the gravitational acceleration, $M = M_{RB} + M_A$ is the inertia matrix due to rigid body M_{RB} and added mass due to hydrodynamic loads M_A, where

$$M_{RB} = diag(\mathrm{m}, \mathrm{m}, \mathrm{m}, I_x, I_y, I_z)$$
$$M_A = -diag(X_{\dot{u}}, Y_{\dot{v}}, Z_{\dot{w}}, K_{\dot{p}}, M_{\dot{q}}, N_{\dot{r}}).$$

$D(\nu)$ is the damping matrix, where

$$D(\nu) = -diag(X_{|u|}|u|, Y_{|v|}|v|, Z_{|w|}|w|, K_{|p|}|p|, M_{|q|}|q|, N_{|r|}|r|)$$

and $C(\nu)$ is Coriolis matrix, for more details see (Fossen, 2011). Model parameters for the *Hippocampus* have been identified based on experimental measurements and are shown in Table 1, (Duecker et al., 2018).

Table 1. *Hippocampus* parameters

Parameter	Value	Parameter	Value
m	$1.43kg$	$K_{\dot{p}}$	$-0.0018kgm^2$
I_x	$-0.00241kgm^2$	$M_{\dot{q}} = N_{\dot{r}}$	$-0.0095kgm^2$
I_y	$-0.01072kgm^2$	$X_{\|u\|}$	$-4.56kg/m$
I_z	$-0.01072kgm^2$	$Y_{\|v\|} = Z_{\|w\|}$	$-17.36kg/m$
$X_{\dot{u}}$	$-1.11kg$	$K_{\|p\|}$	$-0.0028kgm^2$
$Y_{\dot{v}} = Z_{\dot{w}}$	$-2.80kg$	$M_{\|q\|} = N_{\|r\|}$	$-0.0476kgm^2$

Remark. 1 Due to the symmetric shape of the *Hippocampus* and an assumed low speed operation environment ($u_{max} = 1.5m/sec$), some coupling hydrodynamic parameters have been removed to simplify the nonlinear model.

Remark. 2 The buoyancy force is acting on the *Hippocampus* in a point at distance of z_g above its center of gravity, which results in an inverse moment if it rotates around its longitudinal body axis x_B. By this property the roll angle ϕ is kept nearly zero.

3.2 LPV Model

Quasi-LPV representations of nonlinear systems are not unique, and the selection of scheduling parameters affects both synthesis complexity and performance (Kwiatkowski et al., 2006). For the model in equation (6), different LPV models can be obtained based on how scheduling parameter sets are defined. When choosing trigonometric functions, the coupling between position and orientation will be hidden in the parameters, in addition the system will be uncontrollable under this choice of scheduling parameters when they are zero. To avoid these problems, one can use a Taylor series expansion which allows to select the angle itself as a scheduling parameter instead of a trigonometric function (Hoffmann, 2016). As a trade-off between model accuracy and complexity, a second order Taylor expansion is selected. Based on the previous discussion, one can approximate the rotational tensor as

$$\mathcal{G}_{out}:\ \dot{\zeta}_{out} = \left[\begin{array}{c|ccc} 0 & 1-\frac{\psi^2}{4}-\frac{\theta^2}{4}+\frac{\theta^2\psi^2}{4} & -\frac{\psi}{2}+\frac{\psi^3}{6} & \frac{\theta}{2}-\frac{\theta\psi^2}{2}-\frac{\theta^3}{6}+\frac{\theta^3\psi^2}{12} \\ 0 & \frac{\psi}{2}-\frac{\psi\theta^2}{2}-\frac{\psi^3}{6}+\frac{\theta^2\psi^3}{12} & 1-\frac{\psi^2}{4} & \frac{\psi\theta}{3}-\frac{\psi\theta^3}{6}-\frac{\theta\psi^3}{6}+\frac{\theta^3\psi^3}{36} \\ 0 & -\frac{\theta}{2}+\frac{\theta^3}{6} & 0 & 1-\frac{\theta^2}{4} \\ 0 & \frac{-X_{|u|}|u|}{\mathrm{m}-X_{\dot{u}}} & 0 & 0 \\ 0 & 0 & \frac{-Y_{|v|}|v|}{\mathrm{m}-Y_{\dot{v}}} & 0 \\ 0 & 0 & 0 & \frac{-Z_{|w|}|w|}{\mathrm{m}-Z_{\dot{w}}} \end{array}\right]\zeta_{out} + \left[\begin{array}{ccc} 0 & -\frac{u\theta}{4}-\frac{w}{2} & -\frac{u\psi}{4}-\frac{v}{2} \\ 0 & \frac{w\psi}{3} & \frac{u}{2}-\frac{v\psi}{4}+\frac{w\theta}{3} \\ 0 & 0 & -\frac{u}{2}-\frac{w\theta}{4} \\ \frac{1}{\mathrm{m}-X_{\dot{u}}} & 0 & 0 \\ 0 & 0 & 0 \\ 0 & 0 & 0 \end{array}\right]\tau_{out}$$

$$\mathcal{G}_{in}:\ \dot{\zeta}_{in} = \left[\begin{array}{cccccc} 0 & 0 & 0 & 1 & 0 & \theta+\frac{\theta^3}{3} \\ 0 & 0 & 0 & 0 & 1 & 0 \\ 0 & 0 & 0 & 0 & 0 & 1-\frac{\theta^2}{2} \\ z_g\mathrm{mg}(1-\frac{\theta^2}{2}) & 0 & 0 & \frac{-K_{|p|}|p|}{I_x-K_{\dot{p}}} & 0 & 0 \\ 0 & z_g\mathrm{mg}(\theta-\frac{\theta^3}{6}) & 0 & 0 & \frac{-M_{|q|}|q|}{I_y-M_{\dot{q}}} & 0 \\ 0 & 0 & 0 & 0 & 0 & \frac{-N_{|r|}|r|}{I_z-N_{\dot{r}}} \end{array}\right]\zeta_{in} + \left[\begin{array}{ccc} 0 & 0 & 0 \\ 0 & 0 & 0 \\ 0 & 0 & 0 \\ \frac{1}{I_x-K_{\dot{p}}} & 0 & 0 \\ 0 & \frac{1}{I_y-M_{\dot{q}}} & 0 \\ 0 & 0 & \frac{1}{I_z-N_{\dot{r}}} \end{array}\right]\tau_{in} \tag{7}$$

$$\mathcal{R} \approx \begin{bmatrix} 1-\frac{\psi^2}{2}-\frac{\theta^2}{2}+\frac{\theta^2\psi^2}{4} & -\psi+\frac{\psi^3}{6} & \theta-\frac{\theta\psi^2}{2}-\frac{\theta^3}{6}+\frac{\theta^3\psi^2}{12} \\ \psi-\frac{\psi\theta^2}{2}-\frac{\psi^3}{6}+\frac{\theta^2\psi^3}{12} & 1-\frac{\psi^2}{2} & \psi\theta-\frac{\psi\theta^3}{6}-\frac{\theta\psi^3}{6}+\frac{\theta^3\psi^3}{36} \\ -\theta+\frac{\theta^3}{6} & 0 & 1-\frac{\theta^2}{2} \end{bmatrix};$$

and the angular velocity transformation tensor is approximated as

$$\mathcal{T} \approx \begin{bmatrix} 1 & 0 & \theta+\frac{\theta^3}{3} \\ 0 & 1 & 0 \\ 0 & 0 & 1-\frac{\theta^2}{2} \end{bmatrix}.$$

Also, $G(\eta) \approx diag\Big(0,0,0,z_g\mathrm{mg}(1-\frac{\theta^2}{2}), z_g\mathrm{mg}(\theta-\frac{\theta^3}{6}), 0\Big)$. A closer look at the approximated nonlinear equations reveals that terms like $\frac{\psi^2 u}{2}$, $\frac{\psi\theta^3 w}{6}$, ... contain products of state variables, and one needs to decide which variable will be used as state and which one as a scheduling parameter. In an attempt to obtain the model with the most coupling information possible, these terms are divided equally between the state variables, e.g.

$$\frac{\psi^2 u}{2} = \frac{\psi^2}{4}u + \frac{u\psi}{4}\psi$$

Remark. 3 Higher order terms like $\frac{\theta^3\psi^2 w}{12}$, $\frac{\theta^2\psi^3 u}{12}$, ... are not divided due to their low contribution.

The resulting model shows that the position dynamics depend on the orientation states and the thrust force. This makes it possible to decompose the whole system into a position subsystem $\mathcal{G}_{out}$ with state vector $\zeta_{out} = [N\ E\ D\ u\ v\ w]^T$, position control input vector $\tau_{out} = [f\ \theta\ \psi]^T$ and a scheduling parameter vector $\rho_{out} = [\theta\ \psi\ u\ v\ w]^T$, and an orientation subsystem $\mathcal{G}_{in}$ with state vector $\zeta_{in} = [\phi\ \theta\ \psi\ p\ q\ r]^T$, orientation control input vector $\tau_{in} = [\tau_\phi\ \tau_\theta\ \tau_\psi]^T$ and its scheduling parameter vector $\rho_{in} = [\theta\ p\ q\ r]^T$, see Fig. 2. The resulting subsystems can be described in equation (7)

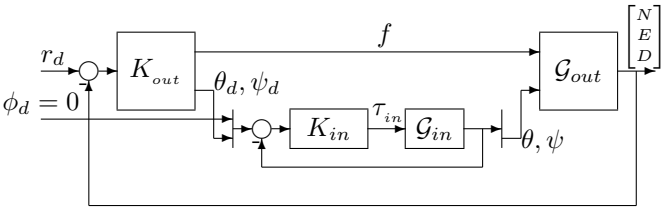

Fig. 2. Cascaded tracking loop for the AUV.

4. FLOCKING CONTROL ARCHITECTURE

Recall the flocking dynamics (Olfati-Saber, 2006)

$$\begin{aligned} \dot{q} &= p \\ \dot{p} &= -\nabla V(q) - (L_{(m)}(q) + cI)p + u^\gamma = U(q,p) \end{aligned} \tag{8}$$

where $V(q)$ is the attraction-repulsion interaction field between agents, $L_{(m)}(q)$ represents the state dependent Laplacian matrix, $c \in \mathbb{R}$ is a friction coefficient and u^γ is an external forcing term, defined as in equation(2), to force the flock to achieve a given mission. Figure 3 represents the proposed loop architecture for a single agent that consists of two modules, a flocking filter block that represents the high-level cooperative control, and a closed-loop agent block that represents the low-level control.

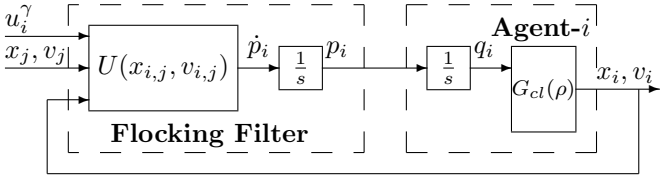

Fig. 3. Agent control architecture loop.

With this architecture, the flocking filter provides each agent i with a reference velocity (p_i), and the agent can track it directly if it is equipped with a velocity tracking controller, or it can track the integral of the reference if it is equipped with a position tracking controller. The overall network dynamics can be written as

$$\begin{aligned} \dot{q} &= p \\ \dot{p} &= -\nabla W(x) - H(x)v \end{aligned} \tag{9}$$

and

$$\begin{bmatrix}\dot{x}\\ \dot{v}\end{bmatrix} = A_{cl}(\rho)\begin{bmatrix}x\\ v\end{bmatrix} + B_{cl}(\rho)q$$
$$y = \begin{bmatrix}x\\ v\end{bmatrix} \tag{10}$$

where $W(x) = V(x)+\mathbf{F}(x)$, $H(x) = L_{(m)}(x)+cI+\nabla^2\mathbf{F}(x)$

Assumptions. We make the following assumptions on the scalar field $F : \mathbb{R}^m \to \mathbb{R}$:

A1 $F : \mathbb{R}^m \to \mathbb{R}$ is convex, twice differentiable and $\exists c_F > 0$ such that it satisfies the Lipschitz condition on the gradient

$$\|\nabla F(q_i)-\nabla F(q_j)\| \leq c_F\|q_i-q_j\| \ \ \forall q_i, q_j \in \mathbb{R}^m \tag{11}$$

We note from the definition of $\mathbf{F}$, that this implies

$$\|\nabla\mathbf{F}(q) - \nabla\mathbf{F}(\tilde{q})\| \leq c_F\|q-\tilde{q}\| \ \ \forall q, \tilde{q} \in \mathbb{R}^{Nm}. \tag{12}$$

A2 $\exists c_V > 0$ such that the flocking interaction potential $V : \mathbb{R}^m \to \mathbb{R}$ satisfies the Lipschitz condition

$$\|\nabla V(q) - \nabla V(\tilde{q})\| \leq c_V\|q-\tilde{q}\| \ \ \forall q, \tilde{q} \in \mathbb{R}^{Nm} \tag{13}$$

Note that the flocking interaction potential proposed in (Olfati-Saber, 2006) does satisfy this condition.

Theorem 2. Under assumptions A1 and A2, if a local controller has been designed for each agent i to achieve a local closed-loop performance such that there exist $\gamma_{out} \geq 0$ that satisfy $\forall p_i \in \mathcal{L}_2$

$$\|e_{q_i}\|^2_{\mathcal{L}_2} \leq \gamma_{out}\|p_i\|^2_{\mathcal{L}_2} \tag{14}$$
$$\|e_{p_i}\|^2_{\mathcal{L}_2} \leq \gamma_{out}\|p_i\|^2_{\mathcal{L}_2} \tag{15}$$

and $c > \Big((c_V + c_F) + (\|L_{(m)}\| + c_F + c)\Big)\gamma_{out}$, the overall dynamics in (9) is stable i.e the trajectories remain bounded for all initial conditions .

Proof Consider the flocking dynamics described in (9). Using the error variables defined above, we can write it as

$$\begin{aligned}\dot{q} &= p\\ \dot{p} &= -\nabla W(q-e_q) - H(x)(p-e_p)\end{aligned} \tag{16}$$

This can be written as

$$\begin{aligned}\dot{q} &= p\\ \dot{p} &= -\nabla W(q) - H(x)(p) + d\end{aligned} \tag{17}$$

where

$$d = \nabla W(q) - \nabla W(q-e_q) + H(x)e_p. \tag{18}$$

Consider the following bounds:

$$\begin{aligned}&\|\nabla W(q) - \nabla W(q-e_q)\| =\\ &\|\nabla V(q) - \nabla V(q-e_q) + \nabla\mathbf{F}(q) - \nabla\mathbf{F}(q-e_q)\|\\ &\leq \|\nabla V(q) - \nabla V(q-e_q)\| + \|\nabla\mathbf{F}(q) - \nabla\mathbf{F}(q-e_q)\|\\ &\leq c_V\|e_q\| + c_F\|e_q\| \leq k_1\|e_q\|\end{aligned} \tag{19}$$

where $k_1 = c_V + c_F$, and

$$\begin{aligned}\|He_p\| &= \|L_{(m)}e_p + \nabla^2\mathbf{F}e_p + ce_p\|\\ &\leq \|L_{(m)}e_p\| + \|\nabla^2\mathbf{F}e_p\| + c\|e_p\|\\ &\leq (\|L_{(m)}\| + c_F + c)\|e_p\| \leq k_2\|e_p\|\end{aligned} \tag{20}$$

where $k_2 = (\|L_{(m)}\| + c_F + c)$. This gives us the following point-wise in time bound on

$$\begin{aligned}\|d(t)\| &\leq k_1\|e_q(t)\| + k_2\|e_p(t)\| \quad \forall t\\ \|d(t)\|^2 &\leq k_1^2\|e_q(t)\|^2 + k_2^2\|e_p(t)\|^2\\ &\quad + 2k_1k_2\|e_q(t)\|\|e_p(t)\| \quad \forall t\end{aligned}$$

Integrating over time, we obtain $\forall T$

$$\begin{aligned}\|d_T\|^2_{\mathcal{L}_2} &\leq k_1^2\|(e_q)_T\|^2_{\mathcal{L}_2} + k_2^2\|(e_p)_T\|^2_{\mathcal{L}_2}\\ &\quad + 2k_1k_2\|(e_q)_T\|_{\mathcal{L}_2}\|(e_p)_T\|_{\mathcal{L}_2}\\ &\leq (k_1^2\gamma_{out}^2 + k_2^2\gamma_{out}^2 + 2k_1k_2\gamma_{out}^2)\|p_t\|^2_{\mathcal{L}_2}\\ &\leq (k_1+k_2)^2\gamma_{out}^2\|p_t\|^2_{\mathcal{L}_2}\end{aligned}$$

Consider the energy function $E : \mathbb{R}_+ \to \mathbb{R}_+$ defined as

$$E(t) := W(q(t)) + \frac{1}{2}p^Tp \tag{21}$$

Differentiating with respect to time, we obtain

$$\begin{aligned}\dot{E}(t) &= \nabla W(q)^Tp + \dot{p}^Tp\\ &= \nabla W(q)^Tp - \nabla W(q)^Tp - p^TH(x)p + d^Tp\\ &= -p^TH(x)p + d^Tp\end{aligned} \tag{22}$$

Integrating on both sides, we have $\forall T > 0$

$$\begin{aligned}E(T) &= E(0) - \int_0^T p(\tau)^TH(x(\tau))p(\tau)d\tau\\ &\quad + \int_0^T d(\tau)^Tp(\tau)d\tau\\ &= E(0) - \int_0^T p^TL_{(m)}pd\tau - \int_0^T p^T\nabla^2\mathbf{F}pd\tau\\ &\quad - c\int_0^T p^Tpd\tau + \int_0^T d^Tpd\tau\\ &\leq E(0) - c\int_0^T p^Tpd\tau + \int_0^T d^Tpd\tau\\ &\leq E(0) - c\|p_T\|^2_{\mathcal{L}_2} + \langle d_T, p_T\rangle\\ &\leq E(0) - c\|p_T\|^2_{\mathcal{L}_2} + \|d_T\|\|p_T\|\\ &\leq E(0) - c\|p_T\|^2_{\mathcal{L}_2} + (k_1+k_2)\gamma_{out}\|p_T\|^2_{\mathcal{L}_2}\\ &\leq E(0) - (c-(k_1+k_2)\gamma_{out})\|p_T\|^2_{\mathcal{L}_2}.\end{aligned} \tag{23}$$

From the conditions of the Theorem $c > (k_1+k_2)\gamma_{out}$, which implies $E(T) \leq E(0)$. Therefore,

$$0 \leq \mathbf{F}(q(T)) \leq E(0) \quad \forall T > 0 \tag{24}$$

which proves the boundedness of trajectories because the level sets of $\mathbf{F}(q)$ are bounded due to convexity.

Remark. 4 Even though the Laplacian L is state dependent (and therefore time varying), an upper bound on $\|L_{(m)}\|$ can be obtained using the maximum degree of an agent which can be calculated for planar graphs($\mathbb{R}^2$) to be 6 and can be estimated for agents living in $\mathbb{R}^3$ (Olfati-Saber, 2006). This can be used for verifying the condition on c as per Theorem 2.

Remark. 5 Asymptotic stability can be shown if a local LPV controller with guaranteed $\mathcal{L}_\infty - \mathcal{L}_\infty$ performance can be designed. This is ongoing work.

5. SIMULATION

5.1 Single Agent Trajectory Tracking

In this subsection, a simulation scenario for trajectory tracking by a single underwater vehicle is shown, based on the loop structure in Fig. 2. The output feedback controller design is based on S/KS loop shaping and the LMI conditions in Theorem 1. This approach aims at shaping the sensitivity using a low-pass filter that

enforces integral action in the loop. In addition, the cut-off frequency of this filter dictates the closed-loop bandwidth while limiting control action by using another high pass filter that constrains control action at low frequencies and enforces roll-off at high frequencies.

Both inner-loop and outer-loop controllers are designed and synthesized based on the approach reviewed in Section 2, taking into account that the inner closed-loop bandwidth ($\omega_{in} = 100 rad/sec$) is chosen to be much faster than the outer closed-loop bandwidth ($\omega_{out} = 1 rad/sec$). The closed-loop sensitivities together with the inverse shaping filters are shown in Fig. 4. The inner-loop controller is designed with performance $\gamma_{in} = 3.27$ and the outer-loop controller has a performance index $\gamma_{out} = 4.06$. Figure 5 shows the trajectory of a *Hippocampus* vehicle that tracks a helix reference with radius of $3m$. The $\mathcal{L}_2$-norm of tracking error is shown in Fig. 6.

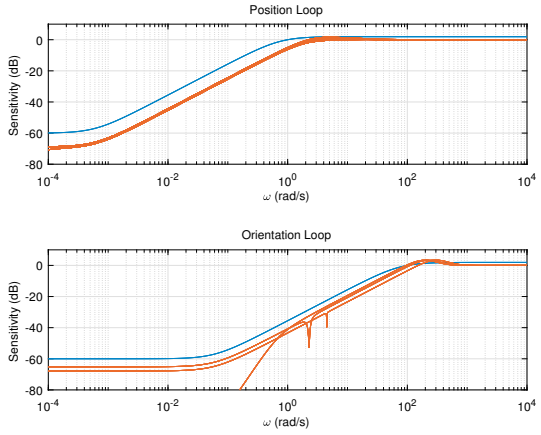

Fig. 4. —Inner and outer loop sensitivities, — inverse of sensitivity shaping filters

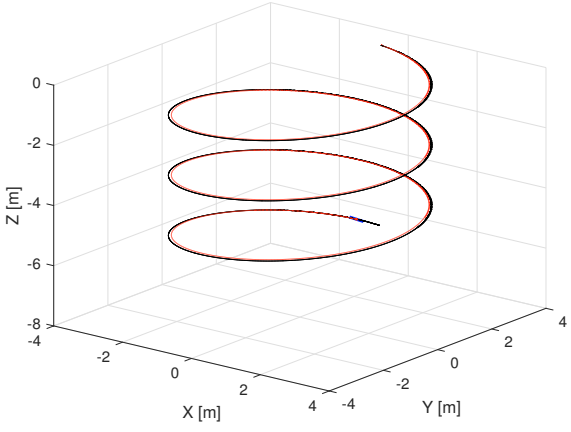

Fig. 5. Trajectory tracking: —reference, — AUV. Link

5.2 Source Seeking Scenario in 3D

To demonstrate the practicality of the proposed approach, this subsection presents a scenario for a swarm of 20 AUVs,

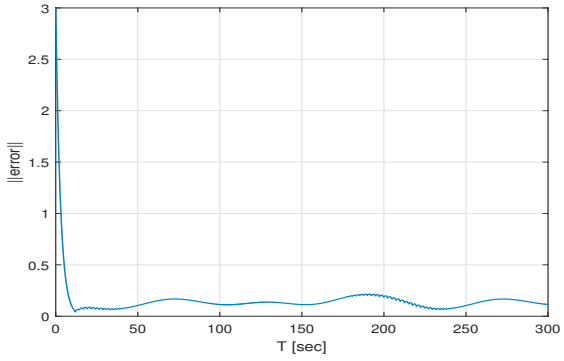

Fig. 6. Tracking error

collaborating to find the source of a three dimensional underwater pollution represented by scalar field $F(x, y, z) = (x-1)^2 + 2(y-8)^2 + 0.5(z-5)^2$ with source located at $(1, 8, 5)$. Agents starts from random initial positions and move through the field up to its origin that represents the source, see Fig. 7. Also, evolution of the algebraic connectivity λ_2 of the resulting interaction graph is shown in Fig. 8.

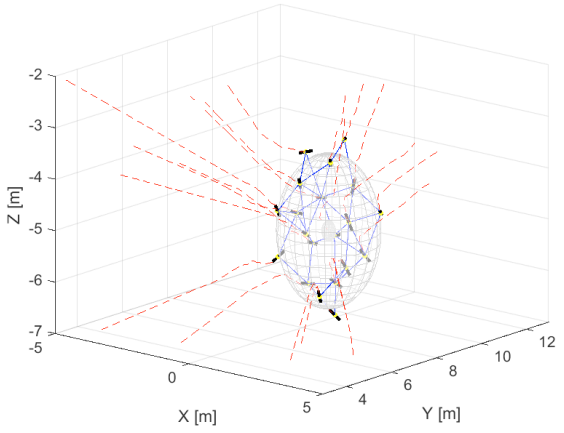

Fig. 7. 3D source seeking with 20 AUVs. Dashed lines represent agents' trajectories; solid lines between agents indicate that there is a communication link. Link

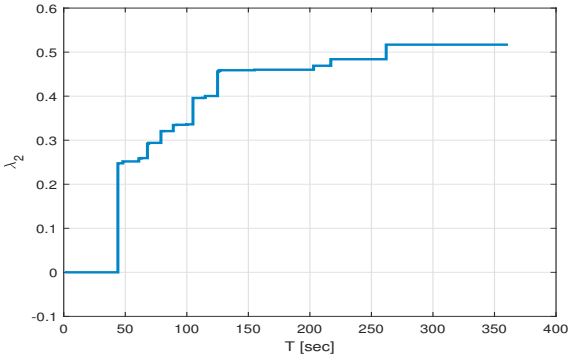

Fig. 8. Evolution of λ_2 for Laplacian graph of AUVs.

Remark. 6 Orientation alignment at the source is not an objective here; it is achieved however while agents are moving, see (Gonzalez et al., 2015).

5.3 Source Seeking Scenario with Multiple Sources

Next we consider planar source seeking (agents move in a fixed z-plane) with 27 agents, in an area on which a field with two sources has been defined. In this case, the *Hippocampus* model can be simplified to move in 2D with inputs of thrusting force and yaw torque, like an LPV model of a dynamic unicycle, see (Attallah and Werner, 2020). The scalar field is defined as $F(x,y) = -exp(-0.01(x+3)^2-0.01(y-12)^2)-exp(-0.02(x-17)^2-0.02(y-5)^2)$ with sources located at $(-3,12)$ and $(17,5)$. The agents start from random initial positions, and they successfully locate the two sources, with two groups of agents forming 2 quasi α-lattices at each source as shown in Fig. 9.

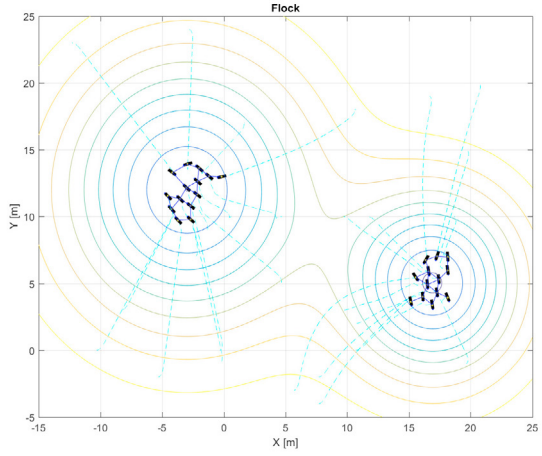

Fig. 9. Planar source seeking with 27 agents. Dashed lines represents agents' trajectories; solid lines between agents indicate that there is a communication link. Link

6. CONCLUSION

This paper presents an extended flocking scheme for a swarm of nonholonomic vehicles, modeled as continuous-time LPV systems. A separation in design enables an efficient design of a local tracking controller for the agents, and of a flocking filter that provides reference trajectories for the agents. The problem of locating a source (extremum) in a convex scalar field is considered, and a sufficient condition for stability of a network of agents is presented. Simulation results demonstrate the practicality of the proposed architecture, which can be applied to realistic networks of mobile robots that are moving in three-dimensional space. Current research is aimed at extending this work to time-varying fields.

REFERENCES

Alvarez, F., Attouch, H., Bolte, J., and Redont, P. (2002). A second-order gradient-like dissipative dynamical system with hessian-driven damping.: Application to optimization and mechanics. *Journal de mathématiques pures et appliquées*, 81(8), 747–779.

Attallah, A. and Werner, H. (2020). Information flow in formation control for nonholonomic agents modeled as lpv system. In *2020 European Control Conference (ECC)*, in press. IEEE.

Barogh, S.A., Rosero, E., and Werner, H. (2015). Formation control of non-holonomic agents with collision avoidance. In *2015 American Control Conference (ACC)*, 757–762. IEEE.

Duecker, D.A., Kreuzer, E., Maerker, G., and Solowjow, E. (2018). Parameter identification for micro underwater vehicles. *PAMM*, 18(1), e201800350.

Fax, J. and Murray, R. (2004). Information flow and cooperative control of vehicle formations. *IEEE Transactions on Automatic Control*, 49(9), 1465–1476.

Fossen, T.I. (2011). *Handbook of marine craft hydrodynamics and motion control*. John Wiley & Sons.

Gonzalez, A.M., Hoffmann, C., and Werner, H. (2015). Lpv formation control for a class of non-holonomic agents with directed and switching communication topologies. In *2015 54th IEEE Conference on Decision and Control (CDC)*, 2792–2797. IEEE.

Hoffmann, C. (2016). *Linear parameter-varying control of systems of high complexity*. Ph.D. thesis, Technische Universität Hamburg.

Kwiatkowski, A., Boll, M.T., and Werner, H. (2006). Automated generation and assessment of affine lpv models. In *Proceedings of the 45th IEEE Conference on Decision and Control*, 6690–6695. IEEE.

Leonard, N.E. and Fiorelli, E. (2001). Virtual leaders, artificial potentials and coordinated control of groups. In *Proceedings of the 40th IEEE Conference on Decision and Control (Cat. No. 01CH37228)*, volume 3, 2968–2973. IEEE.

Olfati-Saber, R. (2006). Flocking for multi-agent dynamic systems: Algorithms and theory. *IEEE Transactions on automatic control*, 51(3), 401–420.

Rosero, E. and Werner, H. (2014). Cooperative source seeking via gradient estimation and formation control (part 2). In *2014 UKACC International Conference on Control (CONTROL)*, 634–639. IEEE.

Soares, J.M., Marjovi, A., Giezendanner, J., Kodiyan, A., Aguiar, A.P., Pascoal, A.M., and Martinoli, A. (2016). Towards 3-d distributed odor source localization: an extended graph-based formation control algorithm for plume tracking. In *2016 IEEE/RSJ International Conference on Intelligent Robots and Systems (IROS)*, 1729–1736. IEEE.

Solowjow, E., Duecker, D., Hackbarth, A., Rausch, V., Geist, A., and Johannink, T. (2018). Hippocampus - project. `https://eugensol.github.io/`.

Turgeman, A., Datar, A., and Werner, H. (2019). Gradient free source-seeking using flocking behavior. In *2019 American Control Conference (ACC)*, 4647–4652. IEEE.

Wu, F. (1995). *Control of Linear Parameter Varying Systems*. Ph.D. thesis, University of California, Berkeley.

Wu, F., Yang, X.H., Packard, A., and Becker, G. (1996). Induced l2-norm control for lpv systems with bounded parameter variation rates. *International Journal of Robust and Nonlinear Control*, 6(9-10), 983–998.